Advancements in Desulfurization process: Fundamentals studies on Selective Separation of Collector-Activated Pyrite from Copper Sulfides

Yesica L. Botero[1,2*], Yann Foucaud [1], Michael Badawi [3], Ricardo Jeldres [2], and Luis A. Cisternas [2,4]

[1] University of Lorraine, GeoRessources Laboratory, France.
[2] Universidad de Antofagasta, Departamento de Ingeniería Química y Procesos de Minerales, Chile.
[3] University of Lorraine, Institut Jean Barriol (IJB), France.
[4] Advanced Mining Technology Center (AMTC), Chile.

*Corresponding author: yesica-lorena.botero@univ-lorraine.fr

Abstract

The desulfurization process is transforming sustainable mining practices. By unlocking the potential of desulfurization for the flotation of all sulfides during the rougher stage, followed by the selective separation of collector-activated pyrite from copper sulfides, this innovative approach enhances mineral recovery while supporting environmentally responsible practices in the mining industry. This study focuses on the intricate surface-chemistry mechanisms essential for effective mineral separation. The role of H_2O_2 on collector-activated pyrite and chalcopyrite was evaluated through adsorption tests, alongside various analyses, including surface chemistry analyses (FTIR and XPS), physical analysis (Z-potential), and chemical analysis through ORP measurements. Two adsorption mechanisms were assessed: collector degradation/desorption and mineral oxidation. The findings reveal that it is possible to reverse the floatability of previously floated pyrite and chalcopyrite by using H_2O_2. The ORP measurements help identify the impact of increasing H_2O_2 concentration on the collector-activated surfaces of pyrite and chalcopyrite. For chalcopyrite, higher H_2O_2 concentrations lead to a transition from a reduced to an oxidized potential. In contrast, the pulp potential of pyrite remains oxidizing, even with increasing H_2O_2 concentrations. These results highlight the importance of controlling H_2O_2 concentration as a pretreatment for the collector-activated pyrite-chalcopyrite system to facilitate selective separation. The FTIR analysis shows the formation of sulfate and carbon dioxide species for pyrite, as well as Cu(II)-hydroxides and oxyhydroxides/sulfate species for chalcopyrite. The Z-potential measurements support these findings; after the minerals were activated and further treated with H_2O_2, the z-potential of pyrite became more negative (-35 mV), likely due to the formation of sulfate anions, while chalcopyrite showed a less negative z-potential (-15 mV), attributed to the formation of oxyhydroxide species. To better understand the oxidation pathways for each mineral, XPS analysis was conducted, revealing insights into the differences in interaction mechanisms between minerals and treatments. For pyrite, the pathways identified include degradation of the alkyl chain (C-C). The proportion of the (C-C) bond in pyrite treated with the collector initially was 13.17%, which decreased to 3.46% following interaction with H_2O_2. Additionally, the formation of sulfates increased from 6.33% (pyrite + collector) to 7.42% (pyrite + collector + H_2O_2). Organo-sulfur species typical of collector decomposition, such as sulfinyl (R_2-SO), were also detected. Pyrite surface oxidation was indicated by shifts in Fe2p 3/2 and Fe2p 1/2 bindings to higher energy levels. For chalcopyrite, the identified pathways included a total transformation of S2p 1/2 leading to the formation of new polysulfide species S_x^{2-} and S_4^{2-}, along with the detection of sulfide and organo-sulfur species. Surface oxidation of chalcopyrite was confirmed through the presence of Fe^{3+}. These findings provide valuable insights into the mechanisms of interaction between collector-activated

minerals and their subsequent H_2O_2 pretreatment, establishing crucial parameters for the selective separation of pyrite from copper sulfides in a copper-iron concentrate.

Key words: desulfurization, selective separation, hydrogen peroxide, collector degradation, mineral oxidation, collector desorption.

Introduction

Tailings, a byproduct of copper ore processing, typically contain minerals like pyrrhotite, arsenopyrite, and a significant amount of pyrite. These minerals can generate acid mine drainage (AMD) when exposed to oxygen and water. The potential for AMD depends on the mineral composition and dissolution rates of the waste, making its management a significant challenge for the mining industry. The current waste management strategy is based on End-of-Pipe technology, focusing on mitigating acid mine drainage (AMD) from existing waste [1,2]. Re-processing tailings seems promising, but it often requires extra reagents, energy, and water. Studies have explored the desulfurization of tailings. Nevertheless, mechanical treatments like grinding and agitation are required to remove oxidized species and activate sulfide surfaces [3,4]. Therefore, an effective tailings desulfurization requires various pretreatments to enhance performance. This requirement complicates Re-processing because the desulfurization flotation circuit requires an additional crushing stage, thereby increasing energy consumption and operating costs. This analysis raises some questions regarding the feasibility of Re-processing waste: What specific pretreatments are most effective for removing oxidized species from sulfide minerals? How do the energy and reagent costs of reprocessing tailings compare to potential environmental benefits? Are there alternative strategies beyond Re-processing that could effectively manage AMD in mining waste? The last question highlights the purpose of this research. Framed within the concept of cleaner production, this study proposes implementing the desulfurization process early in the flotation process. This approach allows for the removal of species responsible for AMD at an initial stage of the flotation process, resulting in tailings free from acidifying species. Nevertheless, implementing the desulfurization process presents challenges. The bulk concentrate obtained from desulfurization poses difficulties from a physical-chemical standpoint [5-7]. An alternative method is needed to selectively separate the activated pyrite from the copper sulfide minerals. It is well known that the behavior of pyrite is influenced by the control of pulp potential, which is significantly affected by oxidation levels and pH. These parameters play a critical role in pyrite flotation. Thus, several questions arise concerning the separation of activated pyrite from copper sulfide minerals after desulfurization. What specific alternative procedures can be used to separate activated pyrite from copper sulfide minerals after desulfurization? How do pyrite chemistry and behavior affect the desulfurization process?

Inorganic depressants such as pH modifiers, oxidants, cyanide, and sulfoxyl, and organic depressants including polysaccharide polymers, lignosulfonate, etc, have been implemented to carry out pyrite depression. All these methods of pyrite depression have been carried out considering flotation circuits in which pyrite is first depressed in the concentration process [8,9]. Therefore, implementing this traditional pyrite depression process would not be feasible for the desulfurization process, followed by selective separation, since the pyrite would already be activated due to the initial bulk concentration stage. It is beneficial to explore physical methods such as ultrasonication and regrinding, as well as the use of strong oxidants like hydrogen peroxide (H_2O_2), following the desulfurization process. These approaches can help either to oxidize the mineral surface or decompose collectors after desulfurization. By implementing these methods, a new and clean surface can be

created, making it ready to react with and adsorb depressant reagents, high oxidants, or a combination of both.

The hypothesis of this work is that using hydrogen peroxide (H_2O_2) after desulfurization can reverse the floatability of either pyrite or chalcopyrite. This can be accomplished by either removing the collector or oxidizing the mineral surface to improve depression for selective separation. H_2O_2 treatment helps control adsorption and desorption processes, promoting the oxidation of mineral surfaces and the decomposition of collectors. The goal is to create tailings with low sulfide content. To achieve this goal, we propose to first obtain a bulk concentrate, followed by the selective separation of the principal gangue mineral, pyrite, from other copper sulfides. We aim to address the following questions: What effect does H_2O_2 treatment have on the characteristics of pyrite and chalcopyrite after it has reacted with collectors? What levels of mineral oxidation or collector degradation/desorption can be achieved using H_2O_2 treatment? What operational conditions enable the extraction of pyrite that has been activated in a porphyry copper mineral?

Methodology

The objective of this research is to examine the impact of H_2O_2 pretreatment on the physicochemical behavior of activated pyrite and chalcopyrite. We aim to determine and understand the reaction mechanisms involved using H_2O_2 pretreatment, which may include surface oxidation, collector decomposition/desorption, or both. Additionally, we are investigating the operational conditions that facilitate the selective separation of pyrite that has been activated during the desulfurization process in porphyry copper minerals. The methodology begins with an adsorption test using a potassium amyl xanthate (PAX) collector. This is followed by pretreatment with H_2O_2 to evaluate the adsorption and desorption mechanisms of the collector on the pyrite and chalcopyrite surface. These findings will help identify the optimal parameters and conditions for conducting pyrite and chalcopyrite flotation, along with the subsequent separation of already floated pyrite or chalcopyrite. Various characterization techniques, including Fourier-transform infrared spectroscopy (FT-IR), X-ray photoelectron spectroscopy (XPS), and Zeta potential analysis, were employed to analyze their behaviors.

Adsorption test

Adsorption tests were carried out to study the physical-chemical interactions between the pyrite and chalcopyrite surfaces and the PAX collector, and the effect of the H_2O_2 pretreatment. 1 g of the fine fraction of pyrite and chalcopyrite (-20 μm) was mixed with a PAX solution at 1×10^{-3} mol/L, at natural pH. After 15 minutes of stirring, the slurry was washed once with deionized water, filtered, and dried at room temperature. Then, after the minerals-PAX interaction, the slurry was filtered, and the activated minerals were mixed with 150 ml of a solution prepared with three different H_2O_2 concentrations (0.001 M, 0.01 M, and 0.1M). Pulp potential and pH were measured during each experiment. After each treatment, the treated slurry was subsequently filtered and dried at room temperature. Zeta Potential, FT-IR, and XPS techniques were used to analyze the powders obtained.

Results

Pulp potential and pH analysis

For the adsorption experiments, six samples were prepared for each mineral, labeled as follows: Treatment 8: mineral; Treatment 7: mineral + PAX; Treatment 5: mineral + H_2O_2 (0.001 M); Treatment 1: mineral H_2O_2 (0.1 M); Treatment 6: mineral + PAX + H_2O_2 (0.001 M); and Treatment 2: mineral + PAX + H_2O_2 (0.1 M). Figure 1 displays the oxidation-reduction potential (ORP) and pH

levels recorded during the experiments investigating the interactions between pyrite and chalcopyrite under various treatments. The study examined three concentrations of H_2O_2 to assess its effects on these mechanisms. The data reveal an interesting trend: as pH decreases, ORP increases. This inverse relationship can be explained by the chemistry involved in the interactions among the minerals, collectors, and hydrogen peroxide. A decrease in pH may result from the formation of acids or other species that release protons (H^+) into the solution. These reactions are often linked to the oxidation of minerals, which produces acidic byproducts. As ORP increases, H_2O_2 decomposes and interacts with other species in the solution, accepting electrons and resulting in a higher ORP. This suggests that the reaction environment is becoming more oxidizing, which can enhance the recovery of certain metals during processing. The role of collectors, such as PAX, is also significant, as they can affect the reactivity of minerals or H_2O_2, thereby influencing both pH and ORP. For instance, as shown in Figure a), samples treated with PAX and followed by H_2O_2 (specifically Py2 and Chpy2) exhibited that higher H_2O_2 concentrations increased mineral potential and enhanced oxidizing pulp potential. Notably, the potential of pyrite remains consistently higher than that of chalcopyrite. At elevated H_2O_2 concentrations, chalcopyrite transitions from a reduced potential to an oxidized state, while at lower concentrations, it continues to significantly affect pyrite, maintaining its oxidizing potential. These findings emphasize the importance of controlling H_2O_2 concentrations for the selective separation of both minerals after collector adsorption. By analyzing the system under high and low concentrations of H_2O_2, we aim to identify optimal conditions for a desulfurization process that selectively separates pyrite from copper sulfides, the primary objective of this research. Consequently, based on the results, this study will focus on two concentrations of H_2O_2: 0.1 M and 0.001 M, anticipating distinct behavioral patterns in mineral interactions. In summary, the observed decrease in pH coupled with an increase in ORP highlights the complex interplay of species formed during the reactions involving minerals, collectors, and H_2O_2, underscoring the need to understand the chemical environment in mineral processing operations, as these dynamics can significantly impact efficiency.

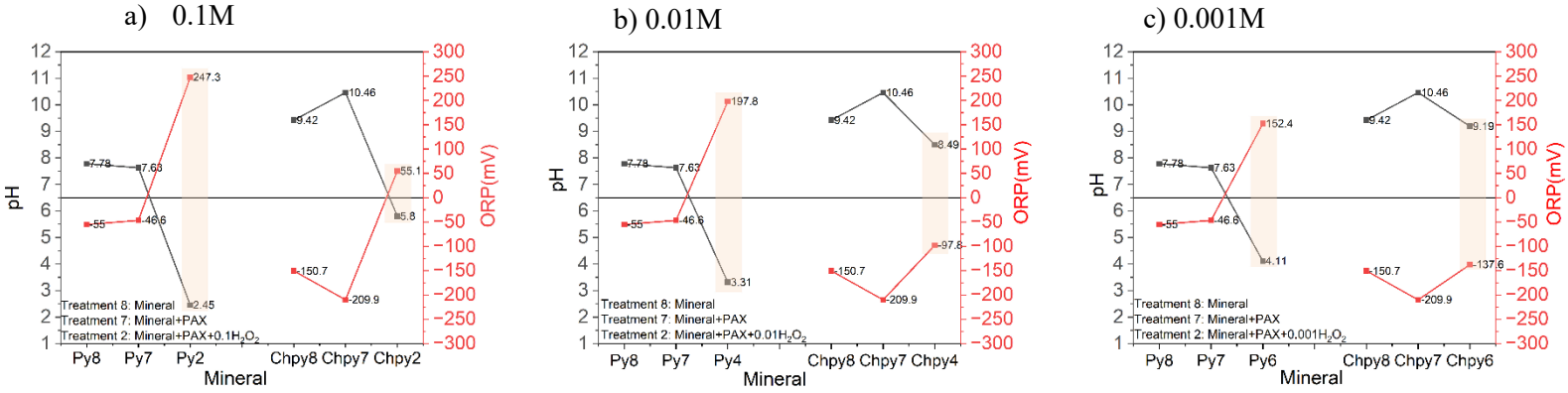

Figure 1. ORP and pH measurements during adsorption tests for pyrite and chalcopyrite under different treatments.

Zeta potential analysis

The zeta potential of the minerals was assessed under three distinct conditions: (1) without any treatment, (2) in contact with the collector, and (3) following H_2O_2 pretreatment. Figure

2 depicts the zeta potential of chalcopyrite and pyrite under these varying conditions. In Figure a), the zeta potential of chalcopyrite interacting with the PAX collector at different H_2O_2 concentrations is illustrated. For chalcopyrite, the isoelectric point (IEP) moves to the right upon collector adsorption, signifying successful adsorption. Conversely, when interacting with peroxide, the IEP shifts to the left from the initial point (Chpy-PAX), suggesting that H_2O_2 may facilitate the removal of the collector rather than oxidizing the mineral surface, as higher isoelectric points evidence oxidative species. It is noteworthy that our primary focus is on the behavior of these minerals at pH 8, as this pH is conducive to initiating desulfurization, which aligns with our research objectives. Furthermore, we will examine pH 11 to determine whether H_2O_2 treatment results in significant changes, as alkaline conditions may enhance selective separation. At pH 8, no significant changes in zeta potential were observed for the chalcopyrite-PAX interactions, whether treated with 0.1 M or 0.001 M H_2O_2. This indicates that at lower concentrations, chalcopyrite is already undergoing oxidation, and increasing the H_2O_2 concentration does not yield substantial changes. In contrast, pyrite exhibited no effect on zeta potential at 0.001 M H_2O_2. Additionally, the figures illustrate the shift in the isoelectric point.

Figure 2b illustrates the results for pyrite, where a comparable analytical approach was employed. The isoelectric point (IEP) exhibited a rightward shift upon collector adsorption. In contrast, interaction with H_2O_2 resulted in a leftward shift of the IEP from its initial position (Py-PAX). This observation suggests that H_2O_2 may promote the removal of the collector rather than oxidizing the mineral surface at the IEP pH, which is approximately 5. At a pH of 8, distinct differences in the behavior of pyrite were observed; the zeta potential exhibited a pronounced shift toward a more negative potential when Py-PAX was in contact with H_2O_2. This behavior is notably different from that of chalcopyrite, which demonstrated a less negative potential. The disparity in these behaviors can be linked to the types of species formed on each mineral's surface. For pyrite, the more negative potential may be attributed to the presence of sulfate species, which enhance negative surface charges. Sulfate is recognized as a stable byproduct formed during the oxidation of pyrite by H_2O_2. In the case of chalcopyrite, the less negative potential may imply the formation of oxidized hydroxides, shifting the potential toward a more oxidative environment (refer to Figure 2c). Finally, Figure 2d depicts the interaction of minerals solely with H_2O_2. The results demonstrate that the interaction of H_2O_2 with the mineral in direct contact differs markedly from scenarios where the collector is first adsorbed and subsequently treated with H_2O_2. These findings confirm that employing peroxide as a pretreatment following desulfurization processes is an effective strategy for eliminating collectors that have already adhered to mineral surfaces, highlighting the distinct behavior compared to prior literature regarding the role and effects of H_2O_2.

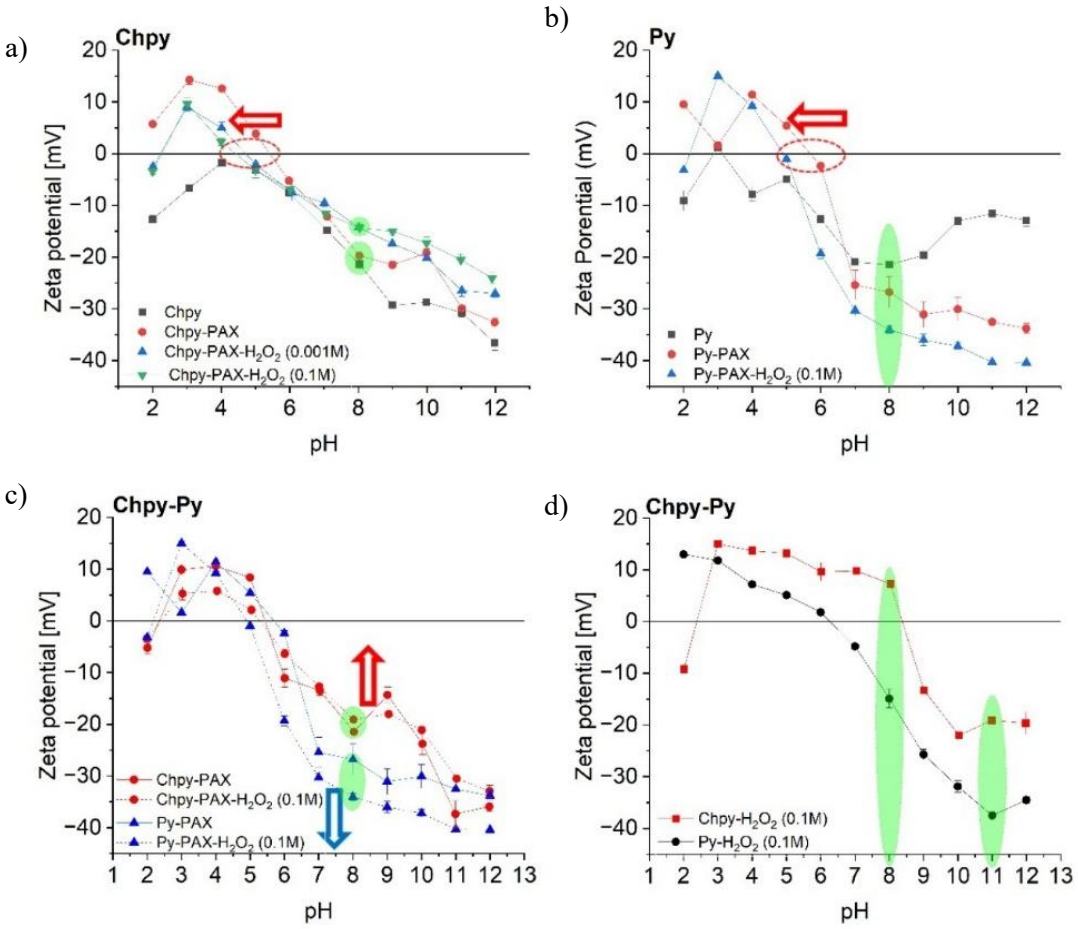

Figure 2. Z-potential measurements for pyrite and chalcopyrite under different treatments.

FT-IR analysis

Figure 3 exhibits the FT-IR spectra of pyrite, pyrite treated with PAX, pyrite+PAX treated with 0.001M, and 0.1 M of H_2O_2. The pyrite+PAX spectrum shows the adsorption of the collector onto the pyrite surface in the region between 3000 and 2800 cm^{-1}. This is related to the -CH group vibration. Also, the region between 1400 and 1000 cm^{-1}shows more interesting interactions between pyrite and PAX, the species Fe-amylxanthate (FeAX) and dixantogen $(AX)_2$. Under COC stretching vibration FeAX it was identified at 1125 cm^{-1} and under C=S stretching vibration, the $(AX)_2$ was identified at 1025 cm^{-1} [10]. This demonstrated the adsorption of PAX collector onto pyrite surface. Then, the pyrite+PAX treated with different H_2O_2 concentrations shows that high H_2O_2 concentrations enable either the collector decomposition of the PAX collector or surface oxidation since the species C=O and O=S=O appear gradually with increasing H_2O_2 concentration. The dominant pathway is not possible to identify here, since the presence of sulfate can come either from collector decomposition or surface oxidation and these signal overlap. So, an XPS study was conducted to figure out the mechanism. Regarding the FTIR spectra of Chalcopyrite, in the region 3000 and 2800 cm^{-1}, the -CH group vibration was absent, demonstrating that the collector does not adhere to this functional group onto the chalcopyrite surface. Instead, the region between 1500 and 500 cm^{-1} shows many interactions between chalcopyrite and PAX, the species Cu-amylxanthate (CuAX), dixantogen $(AX)_2$, and CH_3 were identified, also some more C-S, S-S functional groups, characteristic of PAX collector were

present, demonstrating that the chalcopyrite likely has more interactions through sulfur species rather than alkyl chain of the collector [10]. Besides, in the band around 1375 cm^{-1}, hydroxide, sulfate, and/or sulfite species were present, which overlap. Then, C=O and OH were identified even with the lowest H_2O_2 concentration. These results give insights into the different behavior of the chalcopyrite with the collector and, therefore, when interacting with H_2O_2. Many polysulfide and oxyhydroxide species were formed compared with pyrite. Therefore, the XPS will help to confirm these findings and get more details about the specific mechanisms of each mineral and the treatments.

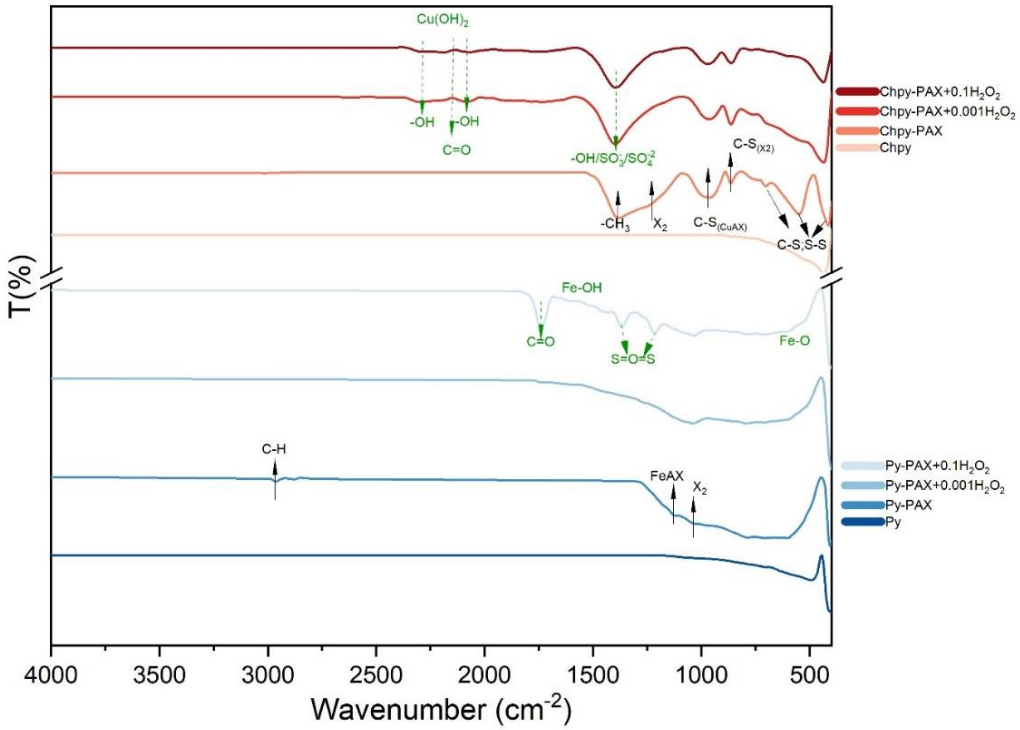

Figure 3. FTIR spectra of pyrite and chalcopyrite before and after treatment with PAX and H_2O_2.

XPS Analysis

To differentiate between collector degradation/desorption and the oxidation of pyrite and chalcopyrite, we analyzed the changes in the carbon (C1s), sulfur (S2p), iron (Fe2p), and copper (Cu2p) spectra for each experiment. Collector degradation is primarily indicated by a decrease in carbon species associated with the collector, such as C-C and C-S species in the C1s spectra, alongside decreases in sulfur species in the S2p spectra. In contrast, the oxidation of pyrite and chalcopyrite would be characterized by an increase in oxidized sulfur and iron species, as well as shifts in binding energies to higher values.

- Collector degradation/desorption in pyrite samples:

Figures 4a-d provide detailed atomic concentrations for the C 1s and S2p spectra of the pyrite samples. The results were used to analyze collector decomposition. The following labels were assigned to the samples assessed: Py 8: Pyrite (Py), Py 7: Pyrite + PAX, Py 5: Pyrite + H_2O_2 (0.001M), Py 1: Pyrite + H_2O_2 (0.1M), Py 6: Pyrite + PAX + H_2O_2 (0.001M), Py 2: Pyrite + PAX + H_2O_2 (0.1M).

- Carbon species and collector decomposition

Adventitious carbon (C-C, C-H components) was present in all samples. This signal is heavily influenced by alkyl-carbon adsorption, which makes it challenging to isolate the collector's alkyl-chain contribution directly. A significant decline in C-C atomic content was observed. The literature suggests that reductions in C-C and C-H components, particularly after H_2O_2 treatment, are not only indicative of collector decomposition but also likely reflect a decrease in adventitious carbon. However, in the samples Py 8, Py 5, and Py 1, the removal of adventitious carbon should be supported by increases in C-O and C=O species; nevertheless, these values do not differ significantly from those of Py 8. To differentiate alkyl chain decomposition from the reduction of adventitious carbon, we assessed the relative decrease in C-C and C-H bonds. The results indicate that when samples were treated first with a collector and then with H_2O_2. For instance, Py 7 displayed a C-C concentration of 13.17%. After treatment with 0.001 M H_2O_2 (Py 6), this value dropped to 6.06%, and with 0.1 M H_2O_2 (Py 6), it further decreased to 3.46% (refer to Figure 4b). This significant reduction suggests that H_2O_2 effectively removes the collector. In the case of Py 2, the C-C-C concentration was even lower than that of Py 1. Moreover, there was an increase in specific oxidized carbon functionalities, such as C-O, C=O, or O-C=O, which correlated with the decreases in C-C and C-H bonds. This could indicate alkyl chain breakdown, a characteristic associated with potassium amyl xanthate (PAX).

Therefore, these results are attributed specifically to the decomposition of the collector's alkyl chain rather than the presence of adventitious carbon. Additionally, the C-S bond (a collector-specific functional group) remained stable across all samples, suggesting that while the alkyl chain is breaking off, the C-S portion remains adsorbed. To explore the underlying mechanism, we also examined the decomposition of the C-S components. The atomic percentage of S2p was assessed, revealing that the mechanisms involved the oxidation of sulfur, leading to the formation of various sulfur-oxygen species.

- Sulfur species and collector decomposition

When samples were treated with a collector followed by H_2O_2 pre-treatment, organosulfur compounds were formed. The oxidation of sulfur in xanthate occurs through direct pathways:

1) Formation of Sulfates (SO_4^{2-}): One of the primary decomposition pathways for sulfur-containing compounds, including xanthates, under strong oxidative conditions such as H_2O_2 treatment, is the oxidation of sulfur to sulfate (SO_4^{2-}):). Figure 4d) illustrates the increase in sulfate levels (Py2) with higher concentrations of H_2O_2, especially compared to Py1 (Py + H_2O_2 0.1M). This indicates that the sulfur atom in the xanthate structure has been fully oxidized.

2) Formation of Organo-Sulfur Species: The detection of specific organo-sulfur species (e.g., sulfinyl, R_2-SO) in the presence of PAX and H_2O_2—compounds that are not typically produced through mineral oxidation alone—provides strong evidence for collector decomposition. These species represent intermediate products resulting from the oxidation of the collector's sulfur while still containing some organic components. Consequently, the oxidation of the C-S bond and the subsequent formation of sulfur-oxygen species (sulfates and organosulfur compounds) signify the breakdown of the active functional group of the xanthate collector.

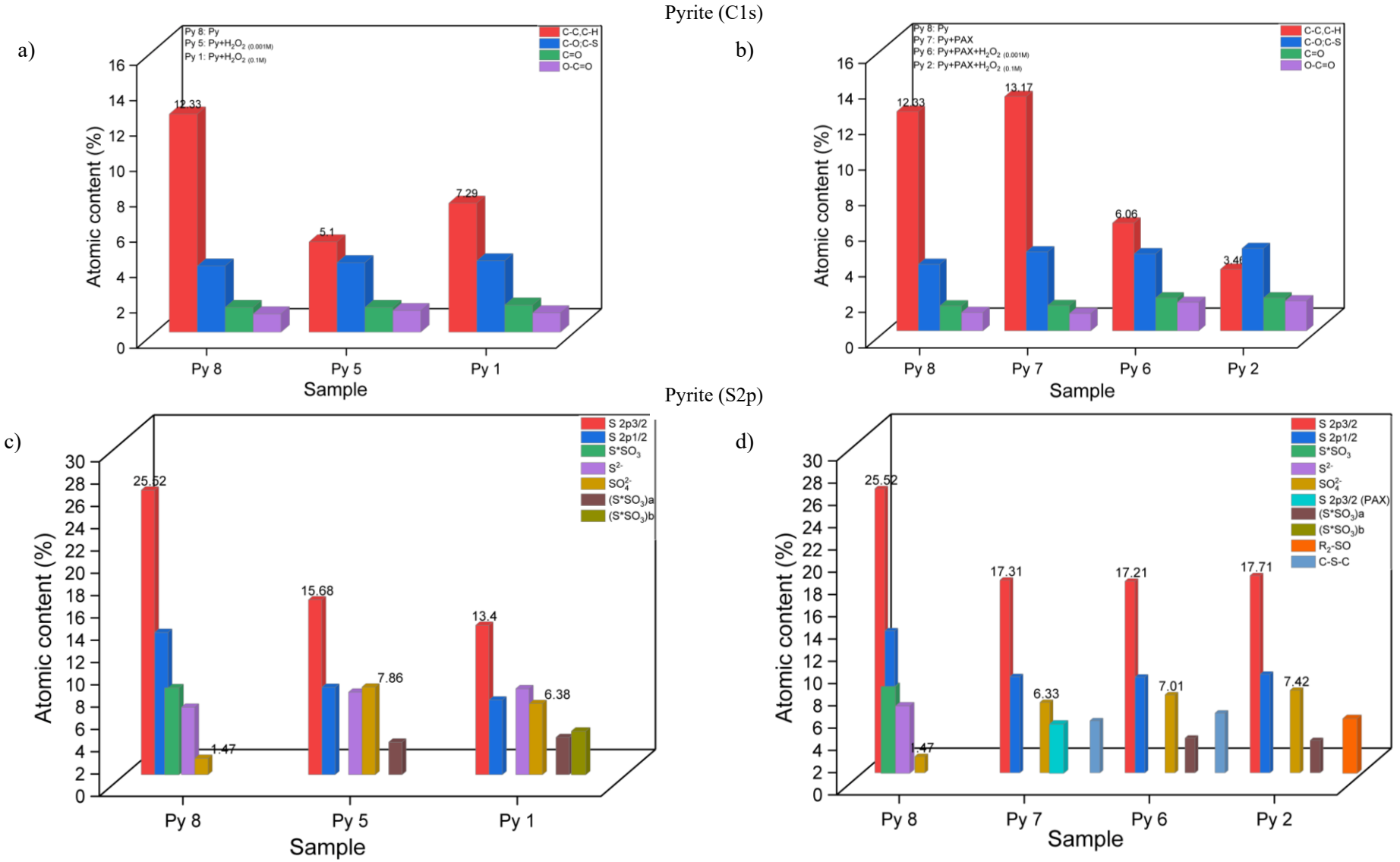

Figure 4. Atomic content percentages of C1s and S2p in high-resolution spectra for pyrite samples

This decomposition leads to a loss of the collector's ability to selectively adsorb onto the mineral surface, thereby reducing its flotation efficiency. The impact of H_2O_2 concentration on these changes was not significantly observed in Py5 and Py6, since the extent of decomposition is often dependent on the concentration of the oxidizing agent. Higher concentrations of H_2O_2 generally result in more complete oxidation of sulfur to higher oxidation states (e.g., organosulfur and sulfate), whereas lower concentrations may yield a mixture of intermediate products, such as sulfites and polysulfides.

- Surface pyrite oxidation

Pyrite exhibits a shift in its binding energy to higher values upon oxidation. Table 1 and Figure 5 illustrate the characteristic band energies S2P and Fe2p for sample Py 8 (Pyrite). These values serve as a baseline for identifying shifts induced by different treatments. The samples evaluated were as follows: Py 7 (pyrite + PAX), Py 6 (pyrite + PAX + H_2O_2 at 0.001 M), and Py 2 (pyrite + PAX + H_2O_2 at 0.1 M). It was observed that the S2p 3/2 and S2p 1/2 bands shifted to higher binding energy with increasing H_2O_2 concentration (+0.31 eV) (refer to Figure 5b and Table 1). A similar trend was noticed for sulfate species. Additionally, new species formed after each pretreatment, such as C-S-C from the collector in Py 7. This band completely shifted to a higher binding energy, indicating the formation of R_2-SO (organosulfur from collector decomposition). This shift demonstrates that the collector was also oxidized through sulfur species. Furthermore, the Fe 2p spectra exhibited the same behavior, with the Fe2p 3/2 and Fe2p 1/2 bands shifting to higher binding energy with higher H_2O_2 concentrations (+0.31 eV) (refer to Figure 5a and Table 1). New species, including Fe-OOH and Fe-O, were formed, indicating the oxidation of pyrite via iron. The formation of sulfate species may result from either the decomposition of the xanthate or reactions with the mineral surface, leading to more complex sulfur structures. This complicates the distinction between surface oxidation and collector oxidation. However, the formation of sulfur trioxide (S^*SO_3) suggests that surface oxidation occurs when H_2O_2 is present at higher concentrations (see Figure 5b and Table 1). In conclusion, based on the atomic percentage and high-resolution spectra results, the plausible pathways for pyrite oxidation initially involve collector decomposition through C-C bond cleavage and C-S oxidation, followed by subsequent surface oxidation.

Table 1. Binding energy shift for pyrite samples

Pyrite								
	S2p					**Fe2p**		
	Binding energy shift (eV)					Binding energy shift (eV)		
Ref:	**S2p 3/2**	**S2p 1/2**	**SO_4^{2-}**	**C-S-C**	**R_2-SO**	**Fe2p 3/2**	**Fe2p 1/2**	**Fe-OOH**
Py 8	**162.82**	**163.96**	**169.04**	**Absent**	**Absent**	**707.44**	**720.43**	**710.39**
Py 7	+0.13	+0.13	+0.3	New	Absent	+0.12	+0.13	+0.47
Py 6	+0.23	+0.24	+0.29	New	Absent	+0.23	+0.24	-0.1
Py 2	+0.31	+0.32	+0.38	Absent	New	+0.31	+0.29	-0.1

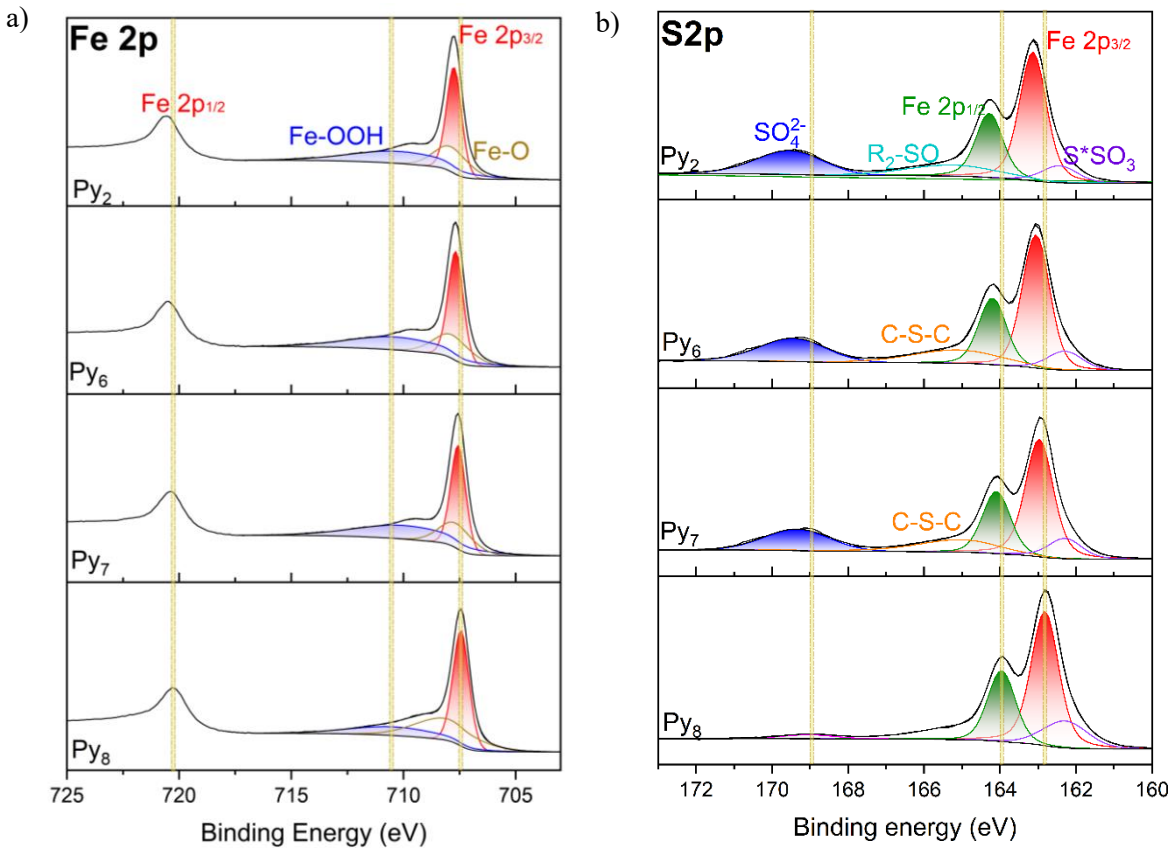

Figure 5. Fe2p and S2p High-resolution spectra for Pyrite samples.

➢ <u>Collector degradation/desorption in chalcopyrite samples:</u>

Figures 6a-d provide detailed atomic concentrations for the C 1s and S2p spectra of the pyrite samples. The results were used to analyze collector decomposition. The following labels were assigned to the samples assessed: Chpy 8: Chpy, Chpy 7: Chpy+PAX, Chpy 5: Chpy+H_2O_2 (0.001M), Chpy 1: Chpy+H_2O_2 (0.1M), Chpy 6: Chpy+PAX+H_2O_2 (0.001M), Chpy 2: Chpy+PAX+H_2O_2 (0.1M).

- Carbon species and collector decomposition

A similar analysis was performed on the chalcopyrite/PAX/H_2O_2 systems. To differentiate between the formation of sulfur species, collector decomposition, and chalcopyrite oxidation, it is essential to examine the changes in sulfur species under various conditions, particularly by comparing samples with and without the collector/H_2O_2. The key observation involves identifying additional or distinct sulfur species that emerge when the collector is present, which go beyond those observed from mineral oxidation alone. Consequently, it is necessary to distinguish between the formation of sulfates, sulfites, and polysulfides resulting from collector decomposition and chalcopyrite oxidation in the presence of H_2O_2. Moreover, additional oxidized sulfur species from the C-S bond—the sulfur component of the collector—were also oxidized. Polysulfides were generated alongside sulfates. The

transformation of sulfur was evident, and the decomposition of the alkyl chain was less significant compared to pyrite.

Figure 6a and 6b show the atomic percentage of C1S for chalcopyrite. There is a decrease in the C-C atomic component; however, it is not as pronounced as for pyrite. Instead, Figures 6c and 6d demonstrate that when the collector has been adsorbed, followed by the interaction with H_2O_2, it produces significantly more intermediate sulfur species than those identified in Figure 6c. This result, combined with the complete transformation observed in the S2p high-resolution spectra (see Figure 7b), indicates that sulfur is transformed into new oxidized species. Comparing Chpy 7 with Chpy 2 makes it clear that the dominant pathway involves S2p oxidation, due to collector decomposition. The decomposition of the collector's C-S bond contributes to the overall pool of sulfur-oxygen species.

Specific Indicators:

1) Increase in Oxidation Products: A higher atomic percentage of sulfates, sulfites, and polysulfides in samples with both PAX and H_2O_2 (e.g., Chpy 2, Chpy 6) compared to samples with only H_2O_2 (e.g., Chpy 1, Chpy 5) indicates that the sulfur from the collector is also being oxidized.

2) Organo-Sulfur Species: The detection of specific organo-sulfur species (e.g., Sulfinyl, R_2-SO) in the presence of PAX and H_2O_2, which are not typically formed through mineral oxidation alone, provides strong evidence for collector decomposition. These species represent intermediate products of the collector's sulfur oxidation while still retaining some organic components.

3) Changes in Polysulfide Peaks: While polysulfides can form from both mineral oxidation and xanthate decomposition, significant shifts in binding energy of these peaks in the presence of the collector can offer valuable insights. The data show polysulfides at 163.96 eV for Chpy 7 (PAX only). In comparison, (S_4^{2-}) polysulfide appears at 162.28 eV for Chpy 2 (PAX + H_2O_2 0.1M), indicating changes in these species due to the interaction of H_2O_2 with the adsorbed collector (refer to Figure 7b and Table 2).

4) The Fe 2p 3/2 and Fe 2p 1/2 spectra indicate that after the collector (Cpy7) was absorbed, the position changed only slightly with each pre-treatment (+0.06 eV). This suggests that the Fe-S binding remains intact. However, new species such as Fe_2O_3, Fe-OOH, and Fe^{3+} were formed, indicating surface oxidation (refer to Figure 7a and Table 2).

5) The Cu 2p 3/2 and Cu 2p 1/2 spectra showed no changes, but new species were formed, including CuO, $CuSO_4$, and Cu(II)-hydroxide. This implies that the Cu-S binding remains stable, but there is evidence of surface oxidation (refer to Figure 7c and Table 2).

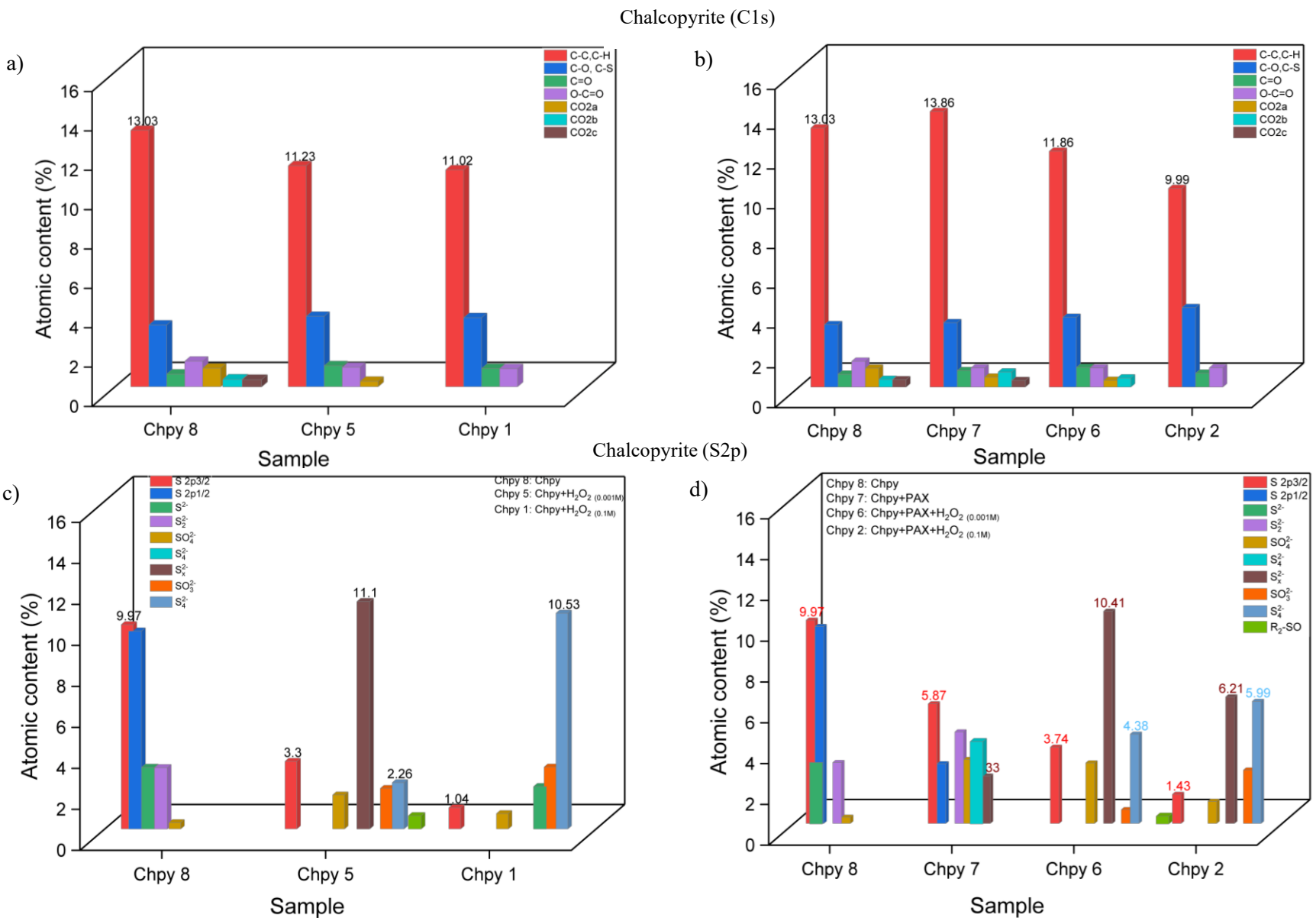

Figure 6. Atomic content percentages of C1s and S2p in high-resolution spectra for Chalcopyrite sample

In conclusion, by systematically comparing the XPS S2p spectra of minerals treated with H_2O_2 alone, those treated with PAX alone, and those treated with both PAX and H_2O_2, we can identify the specific contributions of collector decomposition to the observed sulfur species. The key observation is the presence of new or enhanced oxidized sulfur species, particularly organo-sulfur compounds, that can be uniquely attributed to the breakdown of the sulfur moiety in the collector under oxidative conditions.

Table 2. Binding energy shift for chalcopyrite samples

Chalcopyrite

	S2p						**Fe2p**				
	Binding energy shift (eV)						Binding energy shift (eV)				
Ref:	**S2p 3/2**	**S2p 1/2**	**SO_4^{2-}**	**S_x^{2-}**	**S_4^{2-}**	**R_2-SO**	**Fe2p 3/2**	**Fe2p 1/2**	**Fe_2O_3**	**Fe-OOH**	**Fe2p ½ (Fe^{3+})**
Chpy 8	**161.36**	**162.55**	**169.45**	**Absent**	**Absent**	**Absent**	**707.15**	**720.68**	**711.1**	**Absent**	**723.6**
Chpy 7	+0.03	+0.29	+0.03	New	New	Absent	+0.2	-0.09	+0.19	Absent	+1.1
Chpy 6	+0.02	Absent	+0.32	New	New	New	+0.23	-0.14	+0.22	New	+1.36
Chpy 2	-0.02	Absent	+0.66	New	New	Absent	+0.26	-0.61	+0.16	New	+1.39

	Cu2p					
	Binding energy shift (eV)					
Ref:	**Cu2p 3/2**	**Cu2p 1/2**	**CuO**	**$CuSO_4$**	**Shake up**	**Cu(II)-Hydroxide**
Chpy 8	**938.28**	**952.15**	**932.84**	**935.78**	**Absent**	**954.45**
Chpy 7	+0.09	+0.10	+0.14	+0.36	Absent	+0.11
Chpy 6	+0.13	+0.16	+0.19	+0.19	Absent	+0.02
Chpy 2	+0.05	+0.15	+0.03	-1.57	Absent	+0.05

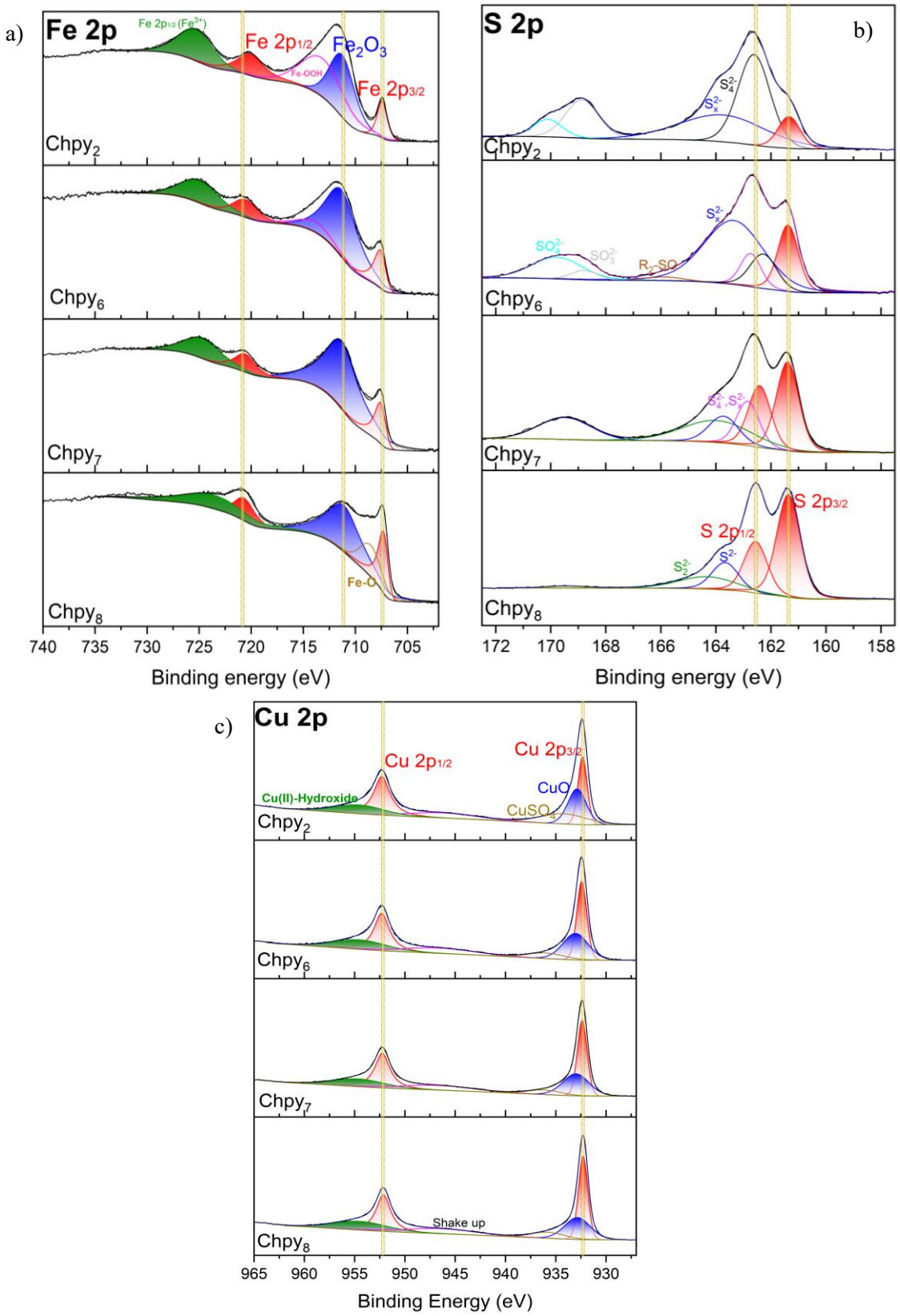

Figure 7. Fe2p, S2p, and Cu2p High-resolution spectra for Chalcopyrite.

Conclusions

In this research, a comprehensive range of characterization techniques was utilized to thoroughly evaluate the effect of H_2O_2 as a pretreatment method for the selective separation of active collector sulfide minerals. Each characterization method was chosen for its ability to provide unique insights, thus enhancing our understanding of how the pulp behaves during flotation processes. Among the techniques employed, zeta potential measurements enabled us to characterize the surface charge properties of the minerals, which play a crucial role in determining their interactions during flotation. FTIR enables the identification of functional groups, such as sulfates and oxyhydroxides, which explains the shift in surface charge as reflected in the Z-potential and also possible differences in the interaction mechanism. Furthermore, because of the complexity of these systems, XPS provides detailed information on the elemental composition and oxidation states of the minerals, thereby shedding light on the fundamental mechanisms that influence flotation behavior. Collectively, these analytical methods provide a multifaceted perspective on the mineral interface, enabling greater control over the flotation process and more efficient mineral recovery. Therefore, the possible pathways for pyrite and chalcopyrite oxidation are as follows:

Pathways for pyrite oxidation:

1) Collector decomposition through: C-C bond cleavage and C-S oxidation.

Specific Indicators:

- A lower atomic percentage of C-C.
- A higher atomic percentage of sulfates.
- Organo-Sulfur species detection (e.g., Sulfinyl, R_2-SO)
- C-S-C detection.

2) Followed by subsequent surface oxidation. Fe2p 3/2 and Fe2p 1/2, and sulfates shift to higher binding energies.

Pathways for chalcopyrite oxidation:

1) Collector decomposition through C-S oxidation.

Specific Indicators:

- Total oxidation of S2p 1/2.
- New polysulfide peaks: S_4^{2-} and S_x^{2-}.
- Organo-Sulfur species detection (e.g., Sulfinyl, R_2-SO)
- Sulfide detection: SO_3^{2-}.

2) Followed by subsequent surface oxidation.

The Fe 2p 3/2 and Fe 2p 1/2 spectra positions changed only slightly with each pre-treatment (+0.06 eV). Nevertheless, new species such as Fe_2O_3, Fe-OOH, and Fe^{3+} were formed. The positions of the Cu 2p 3/2 and Cu 2p 1/2 spectra do not change. But species such as CuO, $CuSO_4$, and Cu(II)-hydroxide were present.

Finally, the key differences in the mechanisms of oxidation between pyrite and chalcopyrite systems lie in: the pyrite system, the dominant mechanisms were the collector degradation through alkyl chain (C-C), and formation of sulfates: SO_4^{2-} followed by surface oxidation through shift to higher binding energy of Fe2p 3/2 and Fe2p 1/2. On the other hand, the dominant mechanism in the chalcopyrite systems was collector degradation, this time through complete transformation of the C-S functional group. The S2p 1/2 transform totally to new polysulfide peaks: S_x^{2-} and S_4^{2-}, sulfide detection and surface oxidation through Fe^{3+}.

Acknowledgments: This publication was supported by Lorraine Université d'Excellence. Agencia Nacional de Investigación y Desarrollo de Chile (ANID), Fondecyt Postdoctoral N° 3240106, ANID/Fondecyt 1211498, ANID/ACT210027, and ANID/AFB23000 . This work was partially done by Luis Cisternas during a visit to the University of Lorraine, supported by MINEDUC-UA project, code ANT22991.

References

1. Blowes, D. W., Ptacek, C. J., Jambor, J. L., Weisener, C. G., Paktunc, D., Gould, W. D., & Johnson, D. B. (2014). The Geochemistry of Acid Mine Drainage. In Treatise on Geochemistry (pp. 131–190). Elsevier. https://doi.org/10.1016/B978-0-08-095975-7.00905-0.
2. Paktunc, A., & Davé, N. (2000). Mineralogy of pyritic waste rock leached by column experiments and prediction of acid mine drainage. In Applied Mineralogy in Research, Economy, Technology, Ecology and Culture, Proceedings of the 6th International Congress on Applied Mineralogy, ICAM, 621–623.
3. Adrianto, L. R., Ciacci, L., Pfister, S., & Hellweg, S. (2023). Toward sustainable reprocessing and valorization of sulfidic copper tailings: Scenarios and prospective LCA. Science of The Total Environment, 871, 162038. https://doi.org/10.1016/j.scitotenv.2023.162038
4. Araya, N., Ramírez, Y., Kraslawski, A., & Cisternas, L. A. (2021). Feasibility of re-processing mine tailings to obtain critical raw materials using real options analysis. Journal of Environmental Management, 284, 112060. https://doi.org/10.1016/j.jenvman.2021.112060
5. Benzaazoua, M., Bouzahzah, H., Taha, Y., Kormos, L., Kabombo, D., Lessard, F., Bussière, B., Demers, I., & Kongolo, M. (2017). Integrated environmental management of pyrrhotite tailings at Raglan Mine: Part 1 challenges of desulphurization process and reactivity prediction. Journal of Cleaner Production, 162, 86–95. https://doi.org/10.1016/j.jclepro.2017.05.161
6. Nadeif, A., Taha, Y., Bouzahzah, H., Hakkou, R., & Benzaazoua, M. (2019). Desulfurization of the Old Tailings at the Au-Ag-Cu Tiouit Mine (Anti-Atlas Morocco). Minerals, 9(7), 401. https://doi.org/10.3390/min9070401
7. Skandrani, A., Demers, I., & Kongolo, M. (2019). Desulfurization of aged gold-bearing mine tailings. Minerals Engineering, 138, 195–203. https://doi.org/10.1016/j.mineng.2019.04.037
8. Cai, J., Jia, X., Ma, Y., Pei, B., Ibrahim, A. M., Su, C., Shen, P., & Liu, D. (2022). Separation of copper-sulfur using sodium polyacrylate as pyrite depressant in acidic pulp: Floatability and adsorption studies. Minerals Engineering, 188, 107815. https://doi.org/10.1016/j.mineng.2022.107815

9. Chapagai, M. K., Fletcher, B., & Gidley, M. J. (2023). Characterization of structure-function properties relevant to copper-activated pyrite depression by different starches. Carbohydrate Polymers, 312, 120841. https://doi.org/10.1016/j.carbpol.2023.120841
10. Botero, Y. L., Canales-Mahuzier, A., Serna-Guerrero, R., López-Valdivieso, A., Benzaazoua, M., & Cisternas, L. A. (2022). Physical-chemical study of IPETC and PAX collector's adsorption on covellite surface. Applied Surface Science, 602. https://doi.org/10.1016/j.apsusc.2022.154232